Journal of Computational Physics **174,** 669–694 (2001)
doi:10.1006/jcph.2001.6932, available online at http://www.idealibrary.com on IDEAL®

The Discrete Geometric Conservation Law and the Nonlinear Stability of ALE Schemes for the Solution of Flow Problems on Moving Grids

Charbel Farhat,* Philippe Geuzaine,* and Céline Grandmont†

*Department of Aerospace Engineering Sciences, Center for Aerospace Structures, University of Colorado at Boulder, Boulder, Colorado 80309-0429; and †CEREMADE, Universite Paris Dauphine, 75775 Paris Cedex 16, France
E-mail: charbel@boulder.colorado.edu

Received December 11, 2000; revised August 13, 2001

Discrete geometric conservation laws (DGCLs) govern the geometric parameters of numerical schemes designed for the solution of unsteady flow problems on moving grids. A DGCL requires that these geometric parameters, which include among others grid positions and velocities, be computed so that the corresponding numerical scheme reproduces exactly a constant solution. Sometimes, this requirement affects the intrinsic design of an arbitrary Lagrangian Eulerian (ALE) solution method. In this paper, we show for sample ALE schemes that satisfying the corresponding DGCL is a necessary and sufficient condition for a numerical scheme to preserve the nonlinear stability of its fixed grid counterpart. We also highlight the impact of this theoretical result on practical applications of computational fluid dynamics.

Key Words: moving schemes; geometric conservation laws; aeroelasticity.

1. INTRODUCTION

In many computational fluid dynamics (CFD) applications, one or many of the boundaries delimiting the physical domain of the flow move in time. Typical examples include flows in reciprocating engines, airfoil oscillations, wing flutter, fighter tail buffeting, aircraft maneuvering, gate sliding, and a large class of free-surface flow problems. When moving boundaries experience large displacements and/or rotations, or when they undergo large deformations, it becomes necessary to solve the flow problem on a moving and possibly deforming grid. Such a grid is often referred to in the literature as a dynamic mesh. Two popular formulations for solving flow problems on dynamic meshes are the closely related

0021-9991/01 $35.00

arbitrary Lagrangian Eulerian (ALE) [2, 3] and dynamic mesh methods [4]. In these and other approaches, a numerical scheme designed for solving the flow equations on moving grids typically incurs the computation of some geometric quantities involving the grid positions and velocities. A useful guideline for evaluating these quantities as well as time-integrating fluxes on moving grids is provided by the enforcement of the so-called discrete geometric conservation law (DGCL) [5]. This law states that the computation of the geometric parameters must be performed in such a way that, independently of the mesh motion, the resulting numerical scheme preserves the state of a uniform flow.

The idea of computing the discrete mesh velocities and other geometric parameters as to preserve a certain physical quantity goes back to the early days of CFD. The terminology "geometric conservation law" was coined in 1979 by Thomas and Lombard [6] who derived this concept from the law of mass conservation in a spatial region bounded by a moving surface, and applied it to construct an improved finite difference method for flow computations on moving grids. This concept was subsequently extended to characterize geometrically conservative schemes as algorithms that preserve the entire state of a uniform flow. First-order, time-accurate, and geometrically conservative ALE finite volume schemes were presented and discussed in [7, 8]. First-order time-accurate and geometrically conservative ALE finite element schemes were presented in [8]. DGCLs for second-order time-accurate ALE finite volume schemes have also been developed and discussed in [9].

There has been sufficient numerical evidence showing that satisfying the DGCL improves considerably the time-accuracy of numerical computations on moving grids [7, 9]. However, for some applications, it has also been reported that respecting or violating the DGCL produced the same numerical results and delivered the same computational performance (for example, see [1]). For this reason, and because the theoretical status of the DGCL has remained for a long time unclear, the following questions have been frequently asked: (a) why should one pay special attention to a uniform flow field, and (b) why should a scheme compute exactly this particular solution of the Navier–Stokes equations when it only approximates the other solutions?

In an attempt to answer the above two questions, Guillard and Farhat have recently performed a theoretical investigation of the DGCL. More specifically, they have proved in [5] that "*for a given scheme that is p-order time-accurate on a fixed mesh, satisfying the corresponding p-discrete geometric conservation law is a sufficient condition for this scheme to be at least first-order time-accurate on a moving mesh.*" Hence, Guillard and Farhat have established that the requirement of computing exactly a uniform field on a moving grid is closely related to an accuracy condition, or at least a consistency condition. While this result sheds some light on the theoretical status of the DGCL, it does not fully explain why it has also been reported that violating the DGCL introduces a weak instability in the numerical solution on moving grids of Euler flows (for example, see [3, 8]).

Motivated by the observations reported in [3, 8] about the effect of the DGCL on numerical stability, Formaggia and Nobile have recently investigated the solution of linear advection–diffusion problems on moving grids by ALE finite element methods [10]. They have shown that for this linear problem, *satisfying the corresponding first-order discrete geometric conservation law is a sufficient condition for the backward Euler implicit scheme to be unconditionally stable*. This new result sheds some light on the relationship between the DGCL and numerical stability, and paves the way for understanding the observations reported in [3, 8]. However, it does not take into account the nonlinearities that characterize

Euler flows, and stops short from predicting the behavior of an ALE scheme when it does not satisfy its corresponding DGCL.

In this paper, we investigate further the theoretical status of the DGCL, and expose its relation to *nonlinear* stability. More specifically, using a d-dimensional nonlinear scalar hyperbolic conservation law (NSCL) as a model problem ($d = 2, 3$), we prove for sample arbitrary Lagrangian Eulerian schemes that *the DGCL requirement corresponds to a necessary and sufficient condition for a numerical scheme to preserve the nonlinear stability of its fixed grid counterpart*. We also highlight the practical importance of this new result on a class of CFD applications.

2. THE ALE MODEL PROBLEM

2.1. Motivation

In this paper, we define stability mainly in terms of spurious oscillations and overshoots. In that sense, nonlinear stability becomes especially vital at shocks and contact discontinuities, which tend to create large spurious oscillations in otherwise stable and monotone solutions.

To date, there exists no perfect nonlinear stability condition for analyzing schemes developed for the solution of the Euler and Navier–Stokes equations. In [13], the author describes nine imperfect conditions of nonlinear stability, each with its own strengths and weaknesses. All but one of these conditions are based on requiring that the solution of the discretized partial differential equation (PDE) inherits some mathematical property of the solution of the continuous PDE that ensures nonlinear stability in the sense defined above. For all but a few of these conditions, the mathematical property of interest can be established only for NSCLs. For the remaining conditions, the relevant nonlinear mathematical property of NSCLs can also be proved for the characteristic variables of the one-dimensional Euler equations. However, none of these nonlinear stability conditions can be mathematically established for the two- and three-dimensional Euler equations. For this reason, NSCLs are often used as model problems for analyzing the nonlinear stability of numerical schemes developed for the solution of the multidimensional Euler equations.

We also note that historically, the potential usefulness of nonlinear stability conditions for equations that do not share the relevant nonlinear properties of NSCLs was demonstrated numerically as early as in Boris and Book [11]. Based on this and other common practice in CFD, we adopt in this paper a d-dimensional ($d = 2, 3$) NSCL as a model problem for analyzing the nonlinear stability of various CFD schemes.

2.2. ALE Form

Because we are interested in flow computations on moving grids, and more specifically, in investigating the relationship between a DGCL and nonlinear stability, we write our model problem in ALE form and consider ALE solution schemes.

For this purpose, we first introduce the concept of an instantaneous configuration $\Omega(x, t) \subset \mathbb{R}^d$, where the coordinates of a point in space are denoted by $x = (x_\beta)_{1\le\beta\le d}$ and time is denoted by t, and that of a reference configuration $\Omega(\xi, 0)$, where the coordinates of a point in space are denoted by $\xi = (\xi_\beta)_{1\le\beta\le d}$ and time is denoted by τ. Next, we define a mapping function between $\Omega(x, t)$ and $\Omega(\xi, 0)$ as follows

$$x = x(\xi, \tau); \quad t = \tau \tag{1}$$

and denote by J its determinant

$$J = det\left(\frac{\partial x}{\partial \xi}\right). \tag{2}$$

From Eqs. (1) and (2), it follows that the ALE form of a typical NSCL

$$\frac{\partial u}{\partial t} + \nabla_x \cdot F(u) = 0 \tag{3}$$

is given by [2]

$$\left.\frac{\partial Ju}{\partial t}\right|_{\xi} + J\nabla_x \cdot (F(u) - wu) = 0 \quad u = u^0 \quad \text{at } t = 0, \tag{4}$$

where

$$\begin{aligned} w &= \left.\frac{\partial x}{\partial t}\right|_{\xi} \\ u &: \mathbb{R}^d \times [0, \infty[\to \mathbb{R} \\ F &= (F_\beta)_{1\le\beta\le d} \\ F_\beta &: \mathbb{R} \to \mathbb{R}. \end{aligned} \tag{5}$$

Equation (4) constitutes our *continuous* model problem.

2.3. Semi-discretization

In this work, we consider the case where the NSCL (4) is semi-discretized by an unstructured finite volume method. However, we also note that the nonlinear stability analysis we present in this paper can be equally performed when the NSCL (4) is semi-discretized by a finite difference or a finite element method. For example, in three dimensions, we assume that $\Omega(x, t)$ is discretized with tetrahedra, and that a dual mesh is constructed with control volumes or cells defined at each vertex as the union of the subtetrahedra resulting from the subdivision by means of the medians of each tetrahedron connected to that vertex.

The semi-discretization of Eq. (4) by a finite volume method can be summarized as follows. Integrating Eq. (4) over a reference cell $\Omega_i(0)$ in the ξ space leads to

$$\frac{d}{dt}\int_{\Omega_i(0)} u\,J\,d\Omega_\xi + \int_{\Omega_i(0)} \nabla_x \cdot (F(u) - wu)\,J\,d\Omega_\xi = 0, \tag{6}$$

which, in view of Eqs. (1) and (2), can be transformed into

$$\frac{d}{dt}\int_{\Omega_i(t)} u\,d\Omega_x + \int_{\Omega_i(t)} \nabla_x \cdot (F(u) - wu)\,d\Omega_x = 0. \tag{7}$$

Integrating by part the second term in the above equation gives

$$\frac{d}{dt}\int_{\Omega_i(t)} u\,d\Omega_x + \int_{\partial\Omega_i(t)} (F(u) - wu) \cdot \mu_i(t)\,ds = 0, \tag{8}$$

where $\mu_i(t)$ denotes the unitary normal to the cell boundary $\partial\Omega_i(t)$.

Let $V(i)$ denote the set of vertices connected to vertex i, and for each $j \in V(i)$, let $\partial\Omega_{ij}(t) = \partial\Omega_i(t) \cap \partial\Omega_j(t)$. The second term in Eq. (8) can be evaluated on an interface-by-interface basis as

$$\int_{\partial\Omega_i(t)} (F(u) - wu) \cdot \mu_i(t)\, ds = \sum_{j \in V(i)} \int_{\partial\Omega_{ij}(t)} (F(u) - wu) \cdot \mu_{ij}(t)\, ds, \tag{9}$$

where $\mu_{ij}(t)$ is the unitary normal to $\partial\Omega_{ij}(t)$. Typically, each term in the above sum is approximated by a numerical flux function Φ—for example, using an (approximate) Riemann solver [12]—in the following manner:

$$\int_{\partial\Omega_{ij}(t)} (F(u) - wu) \cdot \mu_{ij}(t)\, ds \approx |\partial\Omega_{ij}(t)|\ \Phi(u_i, u_j, \nu_{ij}(t), \kappa_{ij}(t)). \tag{10}$$

Here and throughout this paper, $|\cdot|$ denotes the measure of the geometric quantity $(\cdot)$, u_i denotes the *space-average* value of u in the cell $\Omega_i(t)$, and $\nu_{ij}(t)$ and $\kappa_{ij}(t)$ are defined by

$$\nu_{ij}(t) = \frac{1}{|\partial\Omega_{ij}(t)|} \int_{\partial\Omega_{ij}(t)} \mu_{ij}(t)\, ds \tag{11}$$

and

$$\kappa_{ij}(t) = \frac{1}{|\partial\Omega_{ij}(t)|} \int_{\partial\Omega_{ij}(t)} w(t) \cdot \mu_{ij}(t)\, ds. \tag{12}$$

Finally, substituting Eq. (10) into Eq. (8) gives

$$\frac{d}{dt} \int_{\Omega_i(t)} u\, d\Omega_x + \sum_{j \in V(i)} |\partial\Omega_{ij}(t)| \Phi(u_i, u_j, \nu_{ij}(t), \kappa_{ij}(t)) = 0, \tag{13}$$

which completes the description of the semi-discretization of the NSCL (4) by a finite volume method. In general, the numerical flux function Φ is required to be conservative

$$\Phi(u, v, \nu, \kappa) = -\Phi(u, v, -\nu, \kappa) \tag{14}$$

and consistent with the flux function

$$\Phi(u, u, \nu, \kappa) = F(u) \cdot \nu - \kappa u. \tag{15}$$

In summary, Eq. (13) constitutes our *semi-discrete* model problem. Before discussing its time-discretization, we specify next our choice of nonlinear stability condition.

3. CONTINUOUS AND DISCRETE MAXIMUM PRINCIPLES

Among the nine nonlinear stability conditions discussed in [13], the upwind range condition is the strongest. This condition is the easiest to prove and enforce, except possibly at sonic points. It can be interpreted as a local version of the following theorem due to Kruzkhov [14], which is more general than the upwind range condition in the sense that it applies in d spatial dimensions.

THEOREM 3.1 ([14]). *For every measurable and bounded function u^0 in $\mathbb{R}$, there exists one and only one entropic solution of the equation*

$$\begin{gathered}\frac{\partial u}{\partial t}+\sum_{\beta=1}^{d}\frac{\partial f_\beta}{\partial x_\beta}(u,x)=0 \quad x\in\mathbb{R}^d, \quad 0\le t<T\\ u(x,0)=u^0(x) \quad x\in\mathbb{R}^d\end{gathered} \tag{16}$$

in $L^\infty(\mathbb{R}^d\times[0,T[)\cap\mathcal{C}([0,T[;L^1_{loc}(\mathbb{R}^d))$ and this solution verifies the maximum principle

$$\|u\|_{L^\infty(\mathbb{R}^d\times[0,T[)}=\|u^0\|_{L^\infty(\mathbb{R}^d)}. \tag{17}$$

The above theorem states that the solution of a NSCL in d-dimensions satisfies the maximum principle, and therefore is stable in the sense defined in this paper. Therefore, we construct a nonlinear stability condition for numerical schemes by requiring that the solution u_i^n of the semi-discretized NSCL (13) inherits a similar mathematical property—that is, satisfies a similar discrete maximum principle that can be stated as

$$\begin{gathered}\forall u^0 \mid \exists\,(m>0, M>0): m\le u_i^0\le M\ \forall i\\ \Downarrow\\ \forall n\ge 1, \quad m\le u_i^n\le M\ \forall i,\end{gathered} \tag{18}$$

where n is an integer that designates a time station t^n in the temporal domain.

4. TIME-DISCRETIZATION AND DGCLS

4.1. Evaluation of the Flux Function on a Moving Grid

The time integration between t^n and t^{n+1} of the semi-discrete equations (13) raises the issue of where to evaluate the numerical flux function Φ: on the mesh configuration at (x^n,t^n) characterized by v_{ij}^n and κ_{ij}^n, or on that at (x^{n+1},t^{n+1}), or in between these two configurations, or outside these two configurations, or using a combination of all these mesh configurations?

Two approaches have been proposed to address the above issue. In both of these, a sequence of carefully chosen mesh configurations is first identified and evaluated. In the first approach (for example, see [7, 9]), these mesh configurations are used to evaluate some *time-average* values $\overline{v}_{ij}$ and $\overline{\kappa}_{ij}$ of $v_{ij}(t)$ and $\kappa_{ij}(t)$, then a single numerical flux function Φ is computed using $\overline{v}_{ij}$ and $\overline{\kappa}_{ij}$. In the second approach, a numerical flux function is evaluated on each identified mesh configuration, then Φ is computed as the time average of these fluxes (for example, see [3, 8]). In general, the two methodologies lead to different numerical schemes because, for example in the case of a finite volume semi-discretization, Φ is a nonlinear function of $v_{ij}(t)$ and $\kappa_{ij}(t)$. In both methodologies, the averaging coefficients are obtained by requiring that the resulting numerical scheme satisfies its corresponding DGCL. For finite volume methods, the two approaches result in the same averaging coefficients and deliver comparable accuracies; however, the first one is more computationally efficient [9]. For finite element methods, only the second approach has been investigated so far [8].

In this work, we have chosen to semi-discretize our ALE model problem by a finite volume method. Therefore, in view of the above discussion, we consider here the first

approach outlined above for time-integrating the numerical flux function on a moving grid. However, we note that the main result as well as the proofs presented in this paper also hold when the numerical flux function is time integrated on a moving grid by averaging a set of flux functions evaluated on a set of carefully chosen mesh configurations.

4.2. Time Integration

It is important to note that there is no DGCL *per se*: a DGCL is associated with a specific numerical procedure [5]. Therefore, investigating the relationship between the DGCL and nonlinear stability calls not only for specifying the semi-discretization method as done so far, but also for the time-integrator.

In order to address both first- and second-order explicit as well as implicit schemes, we choose here to time integrate the semi-discrete model problem (13) by a θ-scheme. As outlined in Section 4.1, we take into account the effect of moving grids by replacing in Eq. (13) $|\partial\Omega_{ij}(t)|$, $\nu_{ij}(t)$, and $\kappa_{ij}(t)$ by their respective average values $|\overline{\partial\Omega}_{ij}|$, $\bar{\nu}_{ij}$, and $\bar{\kappa}_{ij}$. This leads to the following *discrete* model problem

$$\begin{aligned}\left|\Omega_i^{n+1}\right|u_i^{n+1} = \left|\Omega_i^n\right|u_i^n &- \Delta t\theta \sum_{j\in V(i)} |\overline{\partial\Omega}_{ij}|\Phi\left(u_i^{n+1}, u_j^{n+1}, \bar{\nu}_{ij}, \bar{\kappa}_{ij}\right)\\ &- \Delta t(1-\theta) \sum_{j\in V(i)} |\overline{\partial\Omega}_{ij}|\Phi\left(u_i^{n}, u_j^{n}, \bar{\nu}_{ij}, \bar{\kappa}_{ij}\right),\end{aligned} \tag{19}$$

where $\theta \in [0, 1]$, and for simplicity, a constant time step Δt is assumed. Note that for $\theta = 0$ ($\theta = 1$), one recovers a formulation of the first-order forward (backward) Euler explicit (implicit) scheme on moving grids; for $\theta = \frac{1}{2}$, one recovers a formulation on moving grids of a second-order time-accurate implicit scheme.

As stated in the introduction and in Section 4.1, enforcing the DGCL provides a guideline for designing the sought-after averaging rule, and therefore for determining the values of $|\overline{\partial\Omega}_{ij}|$, $\bar{\nu}_{ij}$, and $\bar{\kappa}_{ij}$. This procedure is discussed next.

4.3. DGCL Based Averaging Rule

Consider first the continuous model problem (4). When this problem admits a constant solution $u = u^* \neq 0$, Eq. (8) becomes

$$\frac{d}{dt}\int_{\Omega_i(t)} d\Omega_x - \int_{\partial\Omega_i(t)} w\cdot\mu_i(t)\,ds = 0, \tag{20}$$

which, in view of Eq. (12), can also be written as

$$\left|\Omega_i^{n+1}\right| - \left|\Omega_i^n\right| = \int_{t^n}^{t^{n+1}} \left(\int_{\partial\Omega_i(t)} w\cdot\mu_i(t)\,ds\right)dt = \sum_{j\in V(i)} \int_{t^n}^{t^{n+1}} |\partial\Omega_{ij}(t)|\kappa_{ij}(t)\,dt. \tag{21}$$

Equation (21) is known as the continuous geometric conservation law (GCL) because it states a conservation property between geometric quantities.

Next, consider the discrete model problem (19). For this system to be able to reproduce exactly the constant solution $u = u^*$, it must satisfy

$$\left|\Omega_i^{n+1}\right|u^* - \left|\Omega_i^n\right|u^* + \Delta t\theta \sum_{j\in V(i)} |\overline{\partial\Omega}_{ij}|\Phi(u^*, u^*, \bar{\nu}_{ij}, \bar{\kappa}_{ij}) + \Delta t(1-\theta) \sum_{j\in V(i)} |\overline{\partial\Omega}_{ij}|\Phi(u^*, u^*, \bar{\nu}_{ij}, \bar{\kappa}_{ij}) = 0. \tag{22}$$

From the consistency condition (15), it follows that

$$\Phi(u^*, u^*, \bar{\nu}_{ij}, \bar{\kappa}_{ij}) = F(u^*)\cdot\bar{\nu}_{ij} - \bar{\kappa}_{ij}u^*, \tag{23}$$

which simplifies Eq. (22) to

$$\left|\Omega_i^{n+1}\right| - \left|\Omega_i^n\right| = \Delta t\frac{F(u^*)}{u^*}\cdot\sum_{j\in V(i)} |\overline{\partial\Omega}_{ij}|\bar{\nu}_{ij} + \Delta t\sum_{j\in V(i)} |\overline{\partial\Omega}_{ij}|\bar{\kappa}_{ij}. \tag{24}$$

However,

$$\sum_{j\in V(i)} |\overline{\partial\Omega}_{ij}|\bar{\nu}_{ij} = 0 \tag{25}$$

because the cells $\Omega_i(t)$ are required to remain closed during the mesh motion. Hence, Eq. (24) simplifies to

$$\left|\Omega_i^{n+1}\right| - \left|\Omega_i^n\right| = \Delta t\sum_{j\in V(i)} |\overline{\partial\Omega}_{ij}|\bar{\kappa}_{ij}, \tag{26}$$

which is the DGCL associated with the numerical scheme (19). Note however that this DGCL is independent of θ. Because the above DGCL (26) resembles the continuous GCL (21), these two geometric conservation laws are unfortunately confused sometimes, and as a consequence the DGCL (26) is sometimes erroneously applied to any ALE scheme.

In summary, the discrete system (19) can preserve the constant solution $u = u^*$ if it satisfies its DGCL (26). This in turn depends on the averaging procedure chosen for computing $|\overline{\partial\Omega}_{ij}|$, $\bar{\kappa}_{ij}$, and $\bar{\nu}_{ij}$. Hence, this averaging procedure is a critical component of an ALE scheme of the form given in (19).

An averaging scheme that respects the DGCL (26) can be designed by exploiting the following observation. The DGCL (26) is the discrete counterpart of the GCL (21), and its left-hand side is identical to the left-hand side of the GCL (21). In other words, the numerical scheme (19) computes exactly the left-hand side of the continuous GCL. Hence, this scheme can be forced to satisfy its DGCL (26) by requiring that it also computes exactly the right-hand side of the continuous GCL—that is,

$$\Delta t\sum_{j\in V(i)} |\overline{\partial\Omega}_{ij}|\bar{\kappa}_{ij} = \int_{t^n}^{t^{n+1}} \left(\int_{\partial\Omega_i(t)} w\cdot\mu_i(t)\,ds\right) dt. \tag{27}$$

In [8, 5], it was shown that if the mesh velocities are constructed to vary linearly inside each face and remain constant in time within $[t^n, t^{n+1}]$—which implies a certain parameterization

of $\mu_i(t)$ and $\mu_{ij}(t)$—the integral $\int_{t^n}^{t^{n+1}} (\int_{\partial\Omega_i(t)} w \cdot \mu_i(t)\, ds)\, dt$ can be computed exactly, and Eq. (26) can be satisfied by computing $|\overline{\partial\Omega}_{ij}|$, $\overline{\kappa}_{ij}$, and $\overline{v}_{ij}$ as

$$|\overline{\partial\Omega}_{ij}| = \frac{1}{\Delta t} \left\| \int_{t^n}^{t^{n+1}} \left(\int_{\partial\Omega_{ij}(t)} \mu_{ij}(t)\, ds \right) dt \right\|_2 \tag{28}$$

$$\overline{\kappa}_{ij} = \kappa(cg_{ij}) \tag{29}$$

$$\overline{v}_{ij} = \frac{1}{|\overline{\partial\Omega}_{ij}|\Delta t} \int_{t^n}^{t^{n+1}} \left(\int_{\partial\Omega_{ij}(t)} \mu_{ij}(t)\, ds \right) dt, \tag{30}$$

where κ denotes the normal component of the mesh velocity w, and cg_{ij} the center of gravity of the face containing the interface $\partial\Omega_{ij}$.

Again, the DGCL requirement provides one guideline among others for computing the average values $|\overline{\partial\Omega}_{ij}|$, $\overline{\kappa}_{ij}$, and $\overline{v}_{ij}$, and therefore completing the specification of an ALE scheme designed for the solution of hyperbolic problems on moving grids. What distinguishes this guideline from others are the following mathematical results. In [5], it was shown that for a given scheme that is p-order time-accurate on a fixed mesh, this requirement is a sufficient condition for this scheme to be at least first-order time-accurate on a moving mesh. In the companion paper [15], it is proved that for multidimensional Euler problems, the extension to moving grids of the classical second-order time-accurate three-point backward difference scheme that was designed in [9] to satisfy its DGCL requirement is also second-order time-accurate on moving grids. Next, we prove that for the NSCL model problem, the DGCL requirement is a necessary and sufficient condition for a numerical scheme constructed on a moving grid to preserve the nonlinear stability in the sense of the discrete maximum principle (18) of its fixed grid counterpart.

5. NONLINEAR STABILITY ANALYSIS

The ALE scheme (19) is an extension to moving grids of the following fixed grid θ-scheme

$$\begin{aligned} u_i^{n+1} = u_i^n &- \frac{\Delta t}{|\Omega_i|}\theta \sum_{j\in V(i)} |\partial\Omega_{ij}|\Phi\left(u_i^{n+1}, u_j^{n+1}, v_{ij}\right) \\ &- \frac{\Delta t}{|\Omega_i|}(1-\theta) \sum_{j\in V(i)} |\partial\Omega_{ij}|\Phi\left(u_i^n, u_j^n, v_{ij}\right). \end{aligned} \tag{31}$$

Since our main objective is to investigate the effect of the DGCL on the nonlinear stability of an ALE scheme such as (19), we consider here the case where the underlying algorithm (31) is stable in the nonlinear sense on fixed grids. To this effect, we assume for example that the numerical flux function is *monotone*, and that it satisfies when required an appropriate CFL condition. We also assume that during the entire mesh motion, the mesh remains valid, that is,

$$\left|\Omega_i^n\right| > 0 \quad \forall n. \tag{32}$$

5.1. First-Order Explicit Time Integration

First, we consider the case $\theta = 0$ for which one obtains the explicit forward Euler ALE scheme

$$\left|\Omega_i^{n+1}\right| u_i^{n+1} = \left|\Omega_i^n\right| u_i^n - \Delta t \sum_{j \in V(i)} |\overline{\partial\Omega}_{ij}| \Phi\left(u_i^n, u_j^n, \overline{\nu}_{ij}, \overline{\kappa}_{ij}\right). \tag{33}$$

Given the identity (25), the above scheme can also be written as

$$\begin{aligned}\left|\Omega_i^{n+1}\right| u_i^{n+1} &= \left|\Omega_i^n\right| u_i^n - \Delta t \sum_{j \in V(i)} |\overline{\partial\Omega}_{ij}| \Phi\left(u_i^n, u_j^n, \overline{\nu}_{ij}, \overline{\kappa}_{ij}\right) + \Delta t \sum_{j \in V(i)} |\overline{\partial\Omega}_{ij}| \overline{\nu}_{ij} \cdot F\left(u_i^n\right) \\ &= \left|\Omega_i^n\right| u_i^n - \Delta t \sum_{j \in V(i)} |\overline{\partial\Omega}_{ij}| \left(\Phi\left(u_i^n, u_j^n, \overline{\nu}_{ij}, \overline{\kappa}_{ij}\right) - F\left(u_i^n\right) \cdot \overline{\nu}_{ij}\right),\end{aligned} \tag{34}$$

and in view of the consistency equation (15), it can be transformed into

$$\begin{aligned}\left|\Omega_i^{n+1}\right| u_i^{n+1} = \left|\Omega_i^n\right| u_i^n &+ \Delta t \left(\sum_{j \in V(i)} |\overline{\partial\Omega}_{ij}| \overline{\kappa}_{ij} \right) u_i^n \\ &- \Delta t \sum_{j \in V(i)} |\overline{\partial\Omega}_{ij}| \left(\Phi\left(u_i^n, u_j^n, \overline{\nu}_{ij}, \overline{\kappa}_{ij}\right) - \Phi\left(u_i^n, u_i^n, \overline{\nu}_{ij}, \overline{\kappa}_{ij}\right)\right).\end{aligned} \tag{35}$$

Let c_{ij} be defined as follows:

$$c_{ij} = \begin{cases} \Delta t \frac{|\overline{\partial\Omega}_{ij}|}{\left|\Omega_i^{n+1}\right|} \frac{\Phi\left(u_i^n, u_j^n, \overline{\nu}_{ij}, \overline{\kappa}_{ij}\right) - \Phi\left(u_i^n, u_i^n, \overline{\nu}_{ij}, \overline{\kappa}_{ij}\right)}{u_i^n - u_j^n} \\ 0 \quad \text{if } u_i^n - u_j^n \end{cases}. \tag{36}$$

For a monotone flux function, c_{ij} satisfies [12]

$$c_{ij} \geq 0. \tag{37}$$

We also assume that

$$\sum_{j \in V(i)} c_{ij} \leq 1, \tag{38}$$

which corresponds to a CFL condition required for the stability on a fixed grid of the basic scheme (31) with $\theta = 0$.

Multiplying and dividing the numerical flux function by $u_i^n - u_j^n$ and dividing Eq. (35) by $|\Omega_i^{n+1}|$ leads after some algebraic manipulations to

$$\begin{aligned}u_i^{n+1} = &\left(1 - \sum_{j \in V(i)} c_{ij}\right) u_i^n + \sum_{j \in V(i)} c_{ij} u_j^n \\ &+ \left(\frac{\left|\Omega_i^n\right| - \left|\Omega_i^{n+1}\right|}{\left|\Omega_i^{n+1}\right|} + \frac{\Delta t}{\left|\Omega_i^{n+1}\right|} \sum_{j \in V(i)} |\overline{\partial\Omega}_{ij}| \overline{\kappa}_{ij} \right) u_i^n.\end{aligned} \tag{39}$$

THEOREM 5.1. *Under assumptions* (37) *and* (38), *satisfying the DGCL* (26) *is a necessary and sufficient condition for the ALE scheme* (39) *to be nonlinearly stable in the sense defined by the discrete maximum principle* (18). *Furthermore, if the consistent ALE scheme* (39) *violates its corresponding DGCL, there exists a constant C such that*

$$\|u^n\|_\infty \le \|u^0\|_\infty e^{C\Delta t T} \quad \forall n \le N = \frac{T}{\Delta t}.$$

Proof. Let

$$g_i^n = \frac{\left|\Omega_i^n\right| - \left|\Omega_i^{n+1}\right|}{\left|\Omega_i^{n+1}\right|} + \frac{\Delta t}{\left|\Omega_i^{n+1}\right|} \sum_{j \in V(i)} |\overline{\partial\Omega}_{ij}| \overline{\kappa}_{ij}. \tag{40}$$

We note that

$$\text{DGCL (26)} \Leftrightarrow g_i^n = 0. \tag{41}$$

Using the above notation, Eq. (39) becomes

$$u_i^{n+1} = \left(1 - \sum_{j \in V(i)} c_{ij}\right) u_i^n + g_i^n u_i^n + \sum_{j \in V(i)} c_{ij} u_j^n, \tag{42}$$

which, in view of (37, 38), implies

$$g_i^n u_i^n + \min\left(u_i^n, \min_{j \in V(i)} u_i^n\right) \le u_i^{n+1} \le \max\left(u_i^n, \max_{j \in V(i)} u_j^n\right) + g_i^n u_i^n. \tag{43}$$

Now, suppose that

$$\forall i, \quad m \le u_i^n \le M. \tag{44}$$

From the inequalities (43) and (44), it follows that

$$\forall i, \quad g_i^n u_i^n + m \le u_i^{n+1} \le M + g_i^n u_i^n, \tag{45}$$

which shows that if the DGCL (26) is satisfied, the discrete maximum principle is also satisfied

$$m \le u_i^{n+1} \le M, \tag{46}$$

and therefore the numerical scheme (39) is nonlinearly stable. This completes the proof that the DGCL (26) is a sufficient condition for the ALE scheme (39) to be stable.

It remains to prove that the DGCL (26) is a necessary condition for the ALE scheme (39) to be nonlinearly stable in the sense of the discrete maximum principle (18). For this purpose, suppose that (39) satisfies the discrete maximum principle (18)—and therefore is nonlinearly stable—and consider the initial condition $u^0 = u^*$, where u^* is some constant field. In that case, $u^* \le u_j^0 \le u^* \forall j$. From (18), it follows that $\forall n \ge 1, u^* \le u_j^n \le u^* \forall j$. This implies that $\forall n \ge 1$, $u_j^n = u^* \forall j$, which means that the numerical scheme (39) preserves the constant solution $u = u^*$. Hence, this scheme satisfies the DGCL (26), which completes

the proof that the DGCL (26) is a necessary condition for the ALE scheme (39) to be stable in the sense of the discrete maximum principle.

Next, we derive an upper bound of the growth in time of the solution of the discrete system (39). First, we note that Eq. (40) can be written as

$$g_i^n = \frac{\Delta t}{\left|\Omega_i^{n+1}\right|}\left(-\frac{1}{\Delta t}\int_{t^n}^{t^{n+1}}\left(\int_{\partial\Omega_i(t)} w\cdot\mu_i(t)\,ds\right)dt + \sum_{j\in V(i)} |\overline{\partial\Omega}_{ij}|\bar{\kappa}_{ij}\right). \tag{47}$$

For any consistent ALE scheme—that is, a scheme that is at least first-order time-accurate—the following result holds:

$$-\frac{1}{\Delta t}\int_{t^n}^{t^{n+1}}\left(\int_{\partial\Omega_i(t)} w\cdot\mu_i(t)\,ds\right)dt + \sum_{j\in V(i)} |\overline{\partial\Omega}_{ij}|\bar{\kappa}_{ij} = O(\Delta t). \tag{48}$$

From Eqs. (47) and (48), it follows that there exists a constant C, which in general depends on w, such that

$$\forall i, \quad \left|g_i^n\right| \le C\Delta t^2. \tag{49}$$

From Eqs. (43) and (49), it also follows that

$$\|u^{n+1}\|_\infty \le \|u^n\|_\infty\left(1+\max_i\left|g_i^n\right|\right) \le \|u^n\|_\infty(1+C\Delta t^2) \tag{50}$$

and therefore

$$\|u^{n+1}\|_\infty \le \|u^0\|_\infty(1+C\Delta t^2)^{n+1}, \tag{51}$$

which finally implies

$$\|u^n\|_\infty \le \|u^0\|_\infty e^{C\Delta t T} \quad \forall\, n \le N = \frac{T}{\Delta t}, \tag{52}$$

where T is the upper limit of the time interval $[0,\ T]$ of interest. Note that the stability estimate (52) is not as sharp as the stability estimate (51), but has a more convenient expression. ■

If the DGCL (26) is satisfied, $g_i^n = 0\ \forall i$, which implies $C = 0$, and therefore

$$\|u^n\|_\infty \le \|u^0\|_\infty. \tag{53}$$

The above stability result, which is similar to that proved in [10] for linear problems, shows that an ALE scheme that satisfies its DGCL is nonlinearly stable independently of the mesh velocity w. This result is of practical interest to many applications such as fluid/structure interaction problems where w is not specified *a priori*, but rather driven by an external medium such as a structure. On the other hand, if the DGCL (26) is not satisfied, the behavior of the ALE scheme (19) as far as stability is concerned depends on the velocity of the moving grid, because the constant C depends on w. Again, the velocity of the dynamic fluid mesh is often dictated by an external agent to the fluid. For this reason, violating the DGCL can restrict significantly the computational time step and

therefore can hamper computational efficiency. Nevertheless, for a smooth mesh motion, if $\Delta t \to 0$ then $e^{C\Delta t T} \to 1$ and numerical stability is recovered. While such a strategy is not computationally efficient, it explains why for sufficiently small time steps, an explicit ALE scheme that violates its DGCL can still behave as well as an explicit ALE scheme that satisfies its DGCL.

5.2. First-Order Implicit Time Integration

Next, we consider the case $\theta = 1$, which leads to the implicit backward Euler ALE scheme

$$\left|\Omega_i^{n+1}\right| u_i^{n+1} = \left|\Omega_i^n\right| u_i^n - \Delta t \sum_{j \in V(i)} |\overline{\partial\Omega}_{ij}| \Phi\left(u_i^{n+1}, u_j^{n+1}, \overline{\nu}_{ij}, \overline{\kappa}_{ij}\right). \tag{54}$$

In this case, we define c_{ij} by

$$c_{ij} = \begin{cases} \Delta t \frac{|\overline{\partial\Omega}_{ij}|}{|\Omega_i^n|} \frac{\Phi\left(u_i^{n+1}, u_j^{n+1}, \overline{\nu}_{ij}, \overline{\kappa}_{ij}\right) - \Phi\left(u_i^{n+1}, u_i^{n+1}, \overline{\nu}_{ij}, \overline{\kappa}_{ij}\right)}{u_i^{n+1} - u_j^{n+1}} \\ 0 \quad \text{if } u_i^{n+1} = u_j^{n+1} \end{cases} \tag{55}$$

and note that for a monotone flux function, c_{ij} satisfies [12]

$$c_{ij} \geq 0. \tag{56}$$

Following the same approach as in the explicit case, we transform (54) into

$$\begin{aligned} &\left(1 + \sum_{j \in V(i)} c_{ij}\right) u_i^{n+1} - \sum_{j \in V(i)} c_{ij} u_j^{n+1} \\ &\quad = u_i^n + \left(\frac{|\Omega_i^n| - \left|\Omega_i^{n+1}\right|}{\left|\Omega_i^n\right|} + \frac{\Delta t}{\left|\Omega_i^n\right|} \sum_{j \in V(i)} |\overline{\partial\Omega}_{ij}| \overline{\kappa}_{ij} \right) u_i^{n+1}. \end{aligned} \tag{57}$$

THEOREM 5.2. *Under assumption* (56), *satisfying the DGCL* (26) *is a necessary and sufficient condition for the ALE scheme* (57) *to be nonlinearly stable in the sense defined by the discrete maximum principle* (18). *Furthermore, if the consistent ALE scheme* (57) *violates its corresponding DGCL, there exists a constant C such that for a sufficiently small time step* Δt

$$\|u^n\|_\infty \leq \|u^0\|_\infty e^{\frac{C\Delta t T}{1 - C\Delta t^2}} \quad \forall\, n \leq N = \frac{T}{\Delta t}.$$

Proof. Here, we define g_i^{n+1} by

$$g_i^{n+1} = \frac{\left|\Omega_i^n\right| - \left|\Omega_i^{n+1}\right|}{\left|\Omega_i^n\right|} + \frac{\Delta t}{\left|\Omega_i^n\right|} \sum_{j \in V(i)} |\overline{\partial\Omega}_{ij}| \overline{\kappa}_{ij}. \tag{58}$$

We remind the reader that for any consistent ALE scheme, there exists a constant C such that

$$\forall i, \quad \left|g_i^{n+1}\right| \leq C \Delta t^2 \tag{59}$$

and note again that

$$\text{DGCL (26)} \Leftrightarrow g_i^{n+1} = 0. \tag{60}$$

Using the above notation, Eq. (57) becomes

$$\left(1 + \sum_{j \in V(i)} c_{ij}\right) u_i^{n+1} - \sum_{j \in V(i)} c_{ij} u_j^{n+1} = u_i^n + g_i^{n+1} u_i^{n+1}. \tag{61}$$

Suppose that the ALE scheme (57) satisfies its DGCL (26). Then, Eq. (61) simplifies to

$$\left(1 + \sum_{j \in V(i)} c_{ij}\right) u_i^{n+1} - \sum_{j \in V(i)} c_{ij} u_j^{n+1} = u_i^n. \tag{62}$$

Let i_m and i_M denote the vertices at which $\min_i u_i^{n+1}$ and $\max_i u_i^{n+1}$ are reached, respectively,

$$u_{i_m}^{n+1} = \min_i u_i^{n+1} \quad u_{i_M}^{n+1} = \max_i u_i^{n+1}. \tag{63}$$

From Eq. (62), it follows that

$$\begin{aligned} \left(1 + \sum_{j \in V(i)} c_{i_m j}\right) u_{i_m}^{n+1} &= \sum_{j \in V(i)} c_{i_m j} u_j^{n+1} + u_{i_m}^n \\ \left(1 + \sum_{j \in V(i)} c_{i_M j}\right) u_{i_M}^{n+1} &= \sum_{j \in V(i)} c_{i_M j} u_j^{n+1} + u_{i_M}^n, \end{aligned} \tag{64}$$

which, in view of (56) and Eq. (63), implies

$$\begin{aligned} \left(1 + \sum_{j \in V(i)} c_{i_m j}\right) \min_i u_i^{n+1} &\geq \left(\sum_{j \in V(i)} c_{i_m j}\right) \min_i u_i^{n+1} + \min_i u_i^n \\ \left(1 + \sum_{j \in V(i)} c_{i_M j}\right) \max_i u_i^{n+1} &\leq \left(\sum_{j \in V(i)} c_{i_M j}\right) \max_i u_i^{n+1} + \max_i u_i^n. \end{aligned} \tag{65}$$

The above inequalities simplify to

$$\begin{aligned} \min_i u_i^{n+1} &\geq \min_i u_i^n \\ \max_i u_i^{n+1} &\leq \max_i u_i^n, \end{aligned} \tag{66}$$

which shows that if the DGCL (26) is satisfied, the discrete maximum principle is also satisfied and therefore the numerical scheme (57) is stable. This completes the proof that the DGCL (26) is a sufficient condition for the ALE scheme (57) to be nonlinearly stable.

The proof that the DGCL (26) is a necessary condition for the ALE scheme (57) to be stable in the sense of the discrete maximum principle is identical to that established in Section 5.1 for the case $\theta = 0$.

Let i_0 denote the vertex at which $\|u^{n+1}\|_\infty$ is reached

$$u_{i_0}^{n+1} = \|u^{n+1}\|_\infty. \tag{67}$$

If the ALE scheme (54) violates its corresponding DGCL (26), from Eqs. (61) and (67) it follows that

$$\left(1 + \sum_{j\in V(i)} c_{i_0 j}\right)\|u^{n+1}\|_\infty \le \left(\sum_{j\in V(i)} c_{i_0 j}\right)\|u^{n+1}\|_\infty + \|u^n\|_\infty + \left|g_{i_0}^{n+1}\right|\|u^{n+1}\|_\infty, \tag{68}$$

which, in view of (59), implies

$$(1 - C\Delta t^2)\|u^{n+1}\|_\infty \le \|u^n\|_\infty. \tag{69}$$

For a time step Δt sufficiently small to have $1 - C\Delta t^2 > 0$, the above inequality is meaningful and results in the following estimate:

$$\|u^n\|_\infty \le \|u^0\|_\infty e^{\frac{C\Delta t T}{1-C\Delta t^2}} \quad \forall n \le N = \frac{T}{\Delta t}. \tag{70}$$

■

Once again, if the DGCL (26) is not satisfied, the stability of the ALE scheme (19) becomes dependent on the velocity of the moving grid via of the constant C. For a smooth mesh motion and a sufficiently small time step ($\Delta t \to 0$), $e^{\frac{C\Delta t T}{1-C\Delta t^2}} \to 1$ and nonlinear stability is recovered. This explains why for sufficiently small time steps, an implicit ALE scheme can exhibit the same stability behavior whether or not it satisfies its corresponding DGCL. However, given that a tiny computational time step is never desirable for an implicit scheme, the above result (70) underscores the importance of satisfying the adequate DGCL.

5.3. Second-Order Implicit Time Integration

In this section, rather than focusing solely on the case $\theta = \frac{1}{2}$ for which the implicit time integrator (19) is formally second-order time-accurate (at least on fixed grids), we consider the more general case where $\theta \in]0, 1[$. We define the two quantities,

$$c_{ij}^k = \begin{cases} \Delta t \frac{|\overline{\partial\Omega}_{ij}|}{|\Omega_\theta|} \frac{\Phi\left(u_i^k, u_j^k \bar{v}_{ij}, \bar{\kappa}_{ij}\right) - \Phi\left(u_i^k, u_i^k, \bar{v}_{ij}, \bar{\kappa}_{ij}\right)}{u_i^k - u_j^k} \\ 0 \quad \text{if } u_i^k = u_j^k \end{cases} \tag{71}$$

and

$$|\Omega_\theta| = \theta\left|\Omega_i^n\right| + (1-\theta)\left|\Omega_i^{n+1}\right| \tag{72}$$

and note that for a monotone flux function, c_{ij}^k satisfies [12]

$$c_{ij}^k \ge 0. \tag{73}$$

We also assume that

$$(1-\theta)\sum_{j\in V(i)} c_{ij}^n \le 1, \tag{74}$$

which corresponds to a CFL condition required for the stability on a fixed grid of the basic scheme (31).

THEOREM 5.3. *Under assumptions* (73) *and* (74), *satisfying the DGCL* (26) *is a necessary and sufficient condition for the ALE scheme* (19) *with* $\theta \in]0,1[$ *to be nonlinearly stable in the sense defined by the discrete maximum principle* (18).

Proof. Suppose that the ALE scheme (19) satisfies its DGCL (26). Then, after similar manipulations to those performed in the cases $\theta = 0$ and $\theta = 1$, the discrete model problem (19) can be transformed into

$$\begin{aligned}\left(1+\theta\sum_{j\in V(i)} c_{ij}^{n+1}\right)u_i^{n+1} - \theta\sum_{j\in V(i)} c_{ij}^{n+1}u_j^{n+1} \\ = \left(1-(1-\theta)\sum_{j\in V(i)} c_{ij}^n\right)u_i^n + (1-\theta)\sum_{j\in V(i)} c_{ij}^n u_j^n.\end{aligned} \tag{75}$$

Let v_i^n be defined as follows:

$$v_i^n = \left(1-(1-\theta)\sum_{j\in V(i)} c_{ij}^n\right)u_i^n + (1-\theta)\sum_{j\in V(i)} c_{ij}^n u_j^n. \tag{76}$$

From the inequalities (73) and (74), it follows that v_i^n is a convex linear combination of u_i^n and u_j^n, $j \in V(i)$. Hence, if u_i^n verifies

$$\forall i, \quad m \le u_i^n \le M, \tag{77}$$

then v_i^n also satisfies

$$\forall i, \quad m \le v_i^n \le M. \tag{78}$$

Next, observe that the discrete system (75) can be written as

$$\left(1+\theta\sum_{j\in V(i)} c_{ij}^{n+1}\right)u_i^{n+1} - \theta\sum_{j\in V(i)} c_{ij}^{n+1}u_j^{n+1} = v_i^n, \tag{79}$$

which is similar to Eq. (62). From (73), (77), (78), and (79) above, it follows that

$$\begin{aligned}\min_i u_i^{n+1} &\ge \min_i v_i^n \ge m \\ \max_i u_i^{n+1} &\le \max_i v_i^n \le M.\end{aligned} \tag{80}$$

Hence, if the DGCL (26) is satisfied, the discrete maximum principle is also satisfied, and therefore the ALE scheme (19) with $\theta \in]0,1[$ is nonlinearly stable. In other words, the DGCL (26) is a sufficient condition for the ALE scheme (19) to be nonlinearly stable.

Finally, we note again that the proof that the DGCL (26) is a necessary condition for the ALE scheme (19) to be stable in the sense of the discrete maximum principle is identical to that established in Section 5.1 for the case $\theta = 0$. ■

6. APPLICATIONS

Here, we illustrate the theoretical result presented in this paper with two academic flow problems, and highlight its impact on practical CFD computations with a real-life aeroelastic application. In all three cases, the fluid is air, which is assumed to be a perfect gas. We also assume that the flow is inviscid, and therefore model it by the three-dimensional Euler equations. The ALE conservative form of these equations is given by

$$\left.\frac{\partial JU}{\partial t}\right|_{\xi} + J\nabla_x \cdot (F(U) - wU) = 0, \tag{81}$$

where U is the fluid state vector, F denotes here the convective fluxes, and the remaining variables have the same meaning as previously.

We semi-discretize the above partial differential equation by a second-order space-accurate finite volume method based on Roe's flux scheme [16]. We achieve second-order spatial accuracy via a piecewise linear interpolation method that follows the principle of the MUSCL (monotonic upwind scheme for conservative laws) procedure [17]. We consider six different implicit time-integration schemes, two of which satisfy their corresponding DGCLs. Before specifying these algorithms, we make the following observations that help introduce a specific notation.

As stated in Section 4.1, the complete description of an ALE scheme such as (19) designed for CFD computations on moving grids requires the specification of the time-averaging procedure employed for computing $|\overline{\partial\Omega}_{ij}|$, $\overline{\nu}_{ij}$, and $\overline{\kappa}_{ij}$. In this work, this averaging procedure can be described as follows (see also [9]). First, a series of mesh configurations denoted by $x^{(m)}$ are identified and evaluated. Then, the nonunitary normals $\tilde{\nu}_{ij}^{(m)}$ associated with these mesh configurations are computed. Finally, $\overline{\tilde{\nu}}_{ij}$ is obtained by averaging the various $\tilde{\nu}_{ij}^{(m)}$ using a specific set of algorithm-dependent weights, $\overline{\nu}_{ij}$ is computed as $\overline{\nu}_{ij} = \overline{\tilde{\nu}}_{ij}/\|\overline{\tilde{\nu}}_{ij}\|_2$ and $|\overline{\partial\Omega}_{ij}|$ is set to $|\overline{\partial\Omega}_{ij}| = \|\overline{\tilde{\nu}}_{ij}\|_2$. Let

$$\Delta t^n = t^{n+1} - t^n, \quad \Delta t^{n-1} = t^n - t^{n-1}, \quad \tau = \frac{\Delta t^n}{\Delta t^{n-1}}$$

$$\alpha_{n+1} = \frac{1+2\tau}{1+\tau}, \quad \alpha_n = -1-\tau, \quad \alpha_{n-1} = \frac{\tau^2}{1+\tau},$$

and let x_{ij} denote here the center of gravity of a *face* of the interface $\partial\Omega_{ij}$. The six implicit time-integration schemes we consider in this section can be summarized as follows.

Scheme A. first-order time-discretization, satisfies its DGCL [8]

$$\left|\Omega_i^{n+1}\right| U_i^{n+1} = \left|\Omega_i^n\right| U_i^n - \Delta t^n \sum_{j\in V(i)} |\overline{\partial\Omega}_{ij}| \Phi\left(U_i^{n+1}, U_j^{n+1}, \overline{\nu}_{ij}, \overline{\kappa}_{ij}\right) \tag{82a}$$

$$x^{(1)} = \frac{1}{2}\left(1 + \frac{1}{\sqrt{3}}\right) x^n + \frac{1}{2}\left(1 - \frac{1}{\sqrt{3}}\right) x^{n+1}$$

$$x^{(2)} = \frac{1}{2}\left(1 - \frac{1}{\sqrt{3}}\right) x^n + \frac{1}{2}\left(1 + \frac{1}{\sqrt{3}}\right) x^{n+1} \tag{82b}$$

$$\begin{aligned}
\overline{\nu}_{ij} &= \frac{1}{2}\big(\nu_{ij}^{(1)} + \nu_{ij}^{(2)}\big) \\
\overline{\kappa}_{ij} &= \frac{1}{2}\left(\frac{x_{ij}^{n+1} - x_{ij}^{n}}{\Delta t^n}\right) \cdot \big(\nu_{ij}^{(1)} + \nu_{ij}^{(2)}\big).
\end{aligned}$$

Scheme B. first-order time-discretization, violates its DGCL [8]

$$\big|\Omega_i^{n+1}\big|\, U_i^{n+1} = \big|\Omega_i^{n}\big| U_i^{n} - \Delta t^n \sum_{j\in V(i)} |\overline{\partial\Omega}_{ij}| \Phi\big(U_i^{n+1}, U_j^{n+1}, \overline{\nu}_{ij}, \overline{\kappa}_{ij}\big) \tag{83a}$$

$$\begin{aligned}
x^{(1)} &= x^n \\
\overline{\nu}_{ij} &= \nu_{ij}^{(1)} \\
\overline{\kappa}_{ij} &= \left(\frac{x_{ij}^{n+1} - x_{ij}^{n}}{\Delta t^n}\right) \times \nu_{ij}^{(1)}.
\end{aligned} \tag{83b}$$

Scheme C. first-order time-discretization, violates its DGCL [8]

$$\big|\Omega_i^{n+1}\big|\, U_i^{n+1} = \big|\Omega_i^{n}\big| U_i^{n} - \Delta t^n \sum_{j\in V(i)} |\overline{\partial\Omega}_{ij}| \Phi\big(U_i^{n+1}, U_j^{n+1}, \overline{\nu}_{ij}, \overline{\kappa}_{ij}\big) \tag{84a}$$

$$\begin{aligned}
x^{(1)} &= x^{n+1} \\
\overline{\nu}_{ij} &= \nu_{ij}^{(1)} \\
\overline{\kappa}_{ij} &= \left(\frac{x_{ij}^{n+1} - x_{ij}^{n}}{\Delta t^n}\right) \times \nu_{ij}^{(1)}
\end{aligned} \tag{84b}$$

Scheme D. second-order time-discretization, satisfies its DGCL [9]

$$\begin{aligned}
\alpha^{n+1}\big|\Omega_i^{n+1}\big|\, U_i^{n+1} = {} & -\alpha^{n}\big|\Omega_i^{n}\big| U_i^{n} - \alpha^{n-1}\big|\Omega_i^{n-1}\big| U_i^{n-1} \\
& - \Delta t^n \sum_{j\in V(i)} |\overline{\partial\Omega}_{ij}| \Phi\big(U_i^{n+1}, U_j^{n+1}, \overline{\nu}_{ij}, \overline{\kappa}_{ij}\big)
\end{aligned} \tag{85a}$$

$$\begin{aligned}
x^{(1)} &= \frac{1}{2}\left(1 + \frac{1}{\sqrt{3}}\right) x^{n-1} + \frac{1}{2}\left(1 - \frac{1}{\sqrt{3}}\right) x^{n} \\
x^{(2)} &= \frac{1}{2}\left(1 - \frac{1}{\sqrt{3}}\right) x^{n-1} + \frac{1}{2}\left(1 + \frac{1}{\sqrt{3}}\right) x^{n} \\
x^{(3)} &= \frac{1}{2}\left(1 + \frac{1}{\sqrt{3}}\right) x^{n} + \frac{1}{2}\left(1 - \frac{1}{\sqrt{3}}\right) x^{n+1} \\
x^{(4)} &= \frac{1}{2}\left(1 - \frac{1}{\sqrt{3}}\right) x^{n} + \frac{1}{2}\left(1 + \frac{1}{\sqrt{3}}\right) x^{n+1} \\
\overline{\nu}_{ij} &= -\frac{\alpha_{n-1}}{2\tau}\big(\nu_{ij}^{(1)} + \nu_{ij}^{(2)}\big) + \frac{\alpha_{n+1}}{2}\big(\nu_{ij}^{(3)} + \nu_{ij}^{(4)}\big) \\
\overline{\kappa}_{ij} &= -\frac{\alpha_{n-1}}{2\tau}\left(\frac{x_{ij}^{n} - x_{ij}^{n-1}}{\Delta t^{n-1}}\right) \cdot \big(\nu_{ij}^{(1)} + \nu_{ij}^{(2)}\big) \\
&\quad + \frac{\alpha_{n+1}}{2}\left(\frac{x_{ij}^{n+1} - x_{ij}^{n}}{\Delta t^n}\right) \cdot \big(\nu_{ij}^{(3)} + \nu_{ij}^{(4)}\big).
\end{aligned} \tag{85b}$$

Scheme E. second-order time-discretization, violates its DGCL [9]

$$\begin{aligned}
\alpha^{n+1}\left|\Omega_i^{n+1}\right| U_i^{n+1} &= -\alpha^n\left|\Omega_i^n\right| U_i^n - \alpha^{n-1}\left|\Omega_i^{n-1}\right| U_i^{n-1} \\
&\quad - \Delta t^n \sum_{j\in V(i)} |\overline{\partial\Omega}_{ij}|\Phi\left(U_i^{n+1}, U_j^{n+1}, \bar{\nu}_{ij}, \bar{\kappa}_{ij}\right) \qquad (86a)\\
x^{(1)} &= x^n \\
\bar{\nu}_{ij} &= \nu_{ij}^{(1)} \qquad (86b)\\
\bar{\kappa}_{ij} &= \left(\frac{x_{ij}^{n+1} - x_{ij}^n}{\Delta t^n}\right)\cdot \nu_{ij}^{(1)}.
\end{aligned}$$

Scheme F. second-order time-discretization, violates its DGCL [9]

$$\begin{aligned}
\alpha^{n+1}\left|\Omega_i^{n+1}\right| U_i^{n+1} &= -\alpha^n\left|\Omega_i^n\right| U_i^n - \alpha^{n-1}\left|\Omega_i^{n-1}\right| U_i^{n-1} \\
&\quad - \Delta t^n \sum_{j\in V(i)} |\overline{\partial\Omega}_{ij}|\Phi\left(U_i^{n+1}, U_j^{n+1}, \bar{\nu}_{ij}, \bar{\kappa}_{ij}\right) \qquad (87a)\\
x^{(1)} &= \frac{1}{2}\left(1+\frac{1}{\sqrt{3}}\right)x^n + \frac{1}{2}\left(1-\frac{1}{\sqrt{3}}\right)x^{n+1} \\
x^{(2)} &= \frac{1}{2}\left(1-\frac{1}{\sqrt{3}}\right)x^n + \frac{1}{2}\left(1+\frac{1}{\sqrt{3}}\right)x^{n+1} \qquad (87b)\\
\bar{\nu}_{ij} &= \frac{1}{2}\left(\nu_{ij}^{(1)} + \nu_{ij}^{(2)}\right) \\
\bar{\kappa}_{ij} &= \frac{1}{2}\left(\frac{x_{ij}^{n+1} - x_{ij}^n}{\Delta t^n}\right)\cdot\left(\nu_{ij}^{(1)} + \nu_{ij}^{(2)}\right).
\end{aligned}$$

Scheme A, Scheme B, and Scheme C, which employ a first-order discretization in time, correspond to the ALE scheme (19) with $\theta = 1$. Scheme D, Scheme E, and Scheme F, which employ a second-order time-discretization, are based on the classical three-point backward difference scheme rather than on (19) with $\theta = \frac{1}{2}$, because the former scheme provides the numerical dissipation that is needed in practical computations, whereas the latter scheme is not dissipative.

Scheme B and Scheme C, which are tempting schemes, violate their respective DGCLs by computing the fluxes on a single mesh configuration rather than the required average configuration. Scheme B uses for that purpose the mesh at time t^n, while Scheme C uses for that purpose the mesh configuration x^{n+1}. Scheme E, which is also a tempting scheme, violates its DGCL not only by computing the fluxes on the single mesh configuration x^n, but also by evaluating the normal component of the mesh velocity simply as $\kappa_{ij} = ((x_{ij}^{n+1} - x_{ij}^n)/\Delta t^n)\cdot\nu_{ij}^n$. On the other hand, Scheme F, which is based on a three-point second-order time-discretization, violates its DGCL by computing the fluxes and evaluating the normal component of the mesh velocity according to the DGCL associated with the two-point second-order time-discretization (19). As stated in Section 4.3, such a scheme is sometimes constructed when the similarity between the GCL (21) and DGCL (26) is confused to erroneously conclude that an ALE scheme should be designed to satisfy the continuous GCL.

6.1. Uniform Flow

First, we consider the case of a one-dimensional uniform flow $U = U^*$ at a Mach number $M_\infty = 0.2$ inside a rigid tube of length $L = 20$ m and a 1 m $\times$ 1 m square cross section. We discretize the computational domain into 200 equally spaced points in the direction x of the flow, and 10 equally spaced points in each of the y- and z-directions. We construct a first mesh by connecting these points with tetrahedra, then generate a second mesh by perturbing randomly the positions of the grid points of the first mesh, without however creating any crossover. Let Δx^0 denote this initial perturbation. Then, we "vibrate" the second mesh according to

$$\Delta x(t) = \Delta x^0 \sin(500\pi t) \tag{88}$$

and compute the time history of the flow using all six schemes outlined above and the vibrating mesh. For each scheme, we compute the relative error

$$RelErr(t^n) = \frac{\|U(t^n) - U^*\|_2}{\|U^*\|_2} \tag{89}$$

and report these errors in Fig. 1 for various values of the computational time step Δt.

The reader can observe that both Scheme A and Scheme D, which satisfy their respective DGCLs, predict exactly the uniform flow. On the other hand, the remaining schemes, which violate their respective DGCLs, exhibit a nonlinear instability that manifests itself in the form of spurious oscillations around the exact solution. The magnitude of these oscillations increases with the computational time step. All these computational results are in perfect agreement with the main theoretical result presented in this paper—that is, satisfying the corresponding DGCL is a necessary and sufficient condition for an ALE scheme to preserve the nonlinear stability in the sense of the discrete maximum principle of its fixed grid counterpart.

Furthermore, the reader can also observe that the exposed oscillations are more important in the cases of Scheme E and Scheme F, which employ a second-order time-discretization, than in that of either Scheme B or Scheme C, which employ a first-order time-discretization. This is an agreement with the conjecture stated in [5] that the higher-order is an ALE scheme on fixed grids, the more important it becomes that it satisfies its DGCL on moving grids.

6.2. Shock Tube

Next, we consider the same tube and flow discretization as in Section 6.1, but initialize the one-dimensional flow with Sod's conditions [18]

$$-\frac{L}{2} \le x < 0 \begin{cases} \rho = 1 \text{ kg/m}^3 \\ p = 10^5 \text{ N/m}^2 \\ v_x = v_y = v_z = 0 \end{cases}$$

$$0 \le x \le \frac{L}{2} \begin{cases} \rho = 0.125 \text{ kg/m}^3 \\ p = 10^4 \text{ N/m}^2 \\ v_x = v_y = v_z = 0 \end{cases}$$

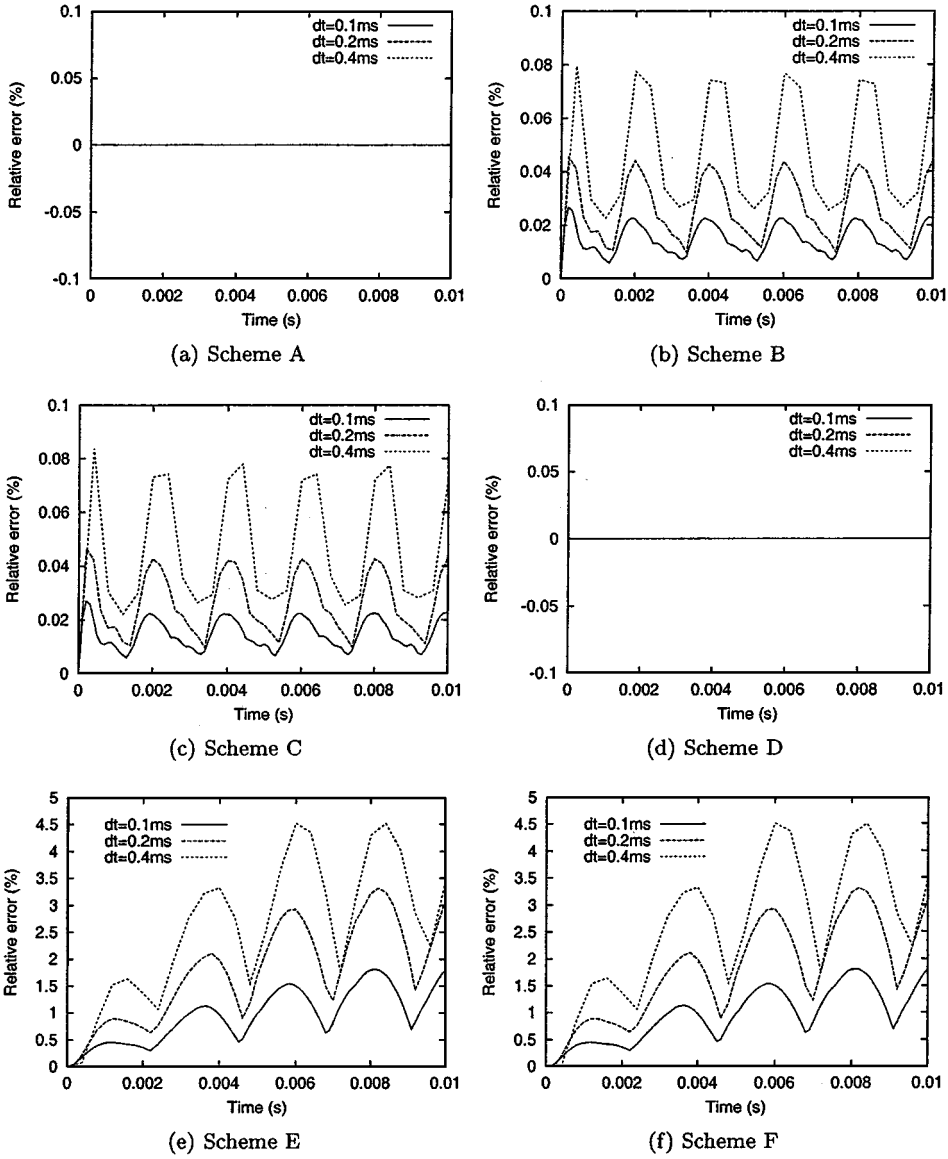

FIG. 1. Uniform flow problem.

and vibrate the mesh according to

$$\Delta x(t) = \Delta x^0 \sin(4000\pi t). \tag{90}$$

We solve this shock tube problem by all six schemes specified above using the same computational time step $\Delta t = 0.05$ ms. This value of Δt corresponds to CFL $= 4$, which is a reasonable compromise between the fact that the shock tube problem is a wave propagation problem and all six schemes employ an implicit time integrator. For each scheme, we report in Fig. 2 the predicted distribution of the density along the x-axis at $t = 10$ ms. Here again, the reader can observe that the schemes that do not satisfy their corresponding DGCLs,

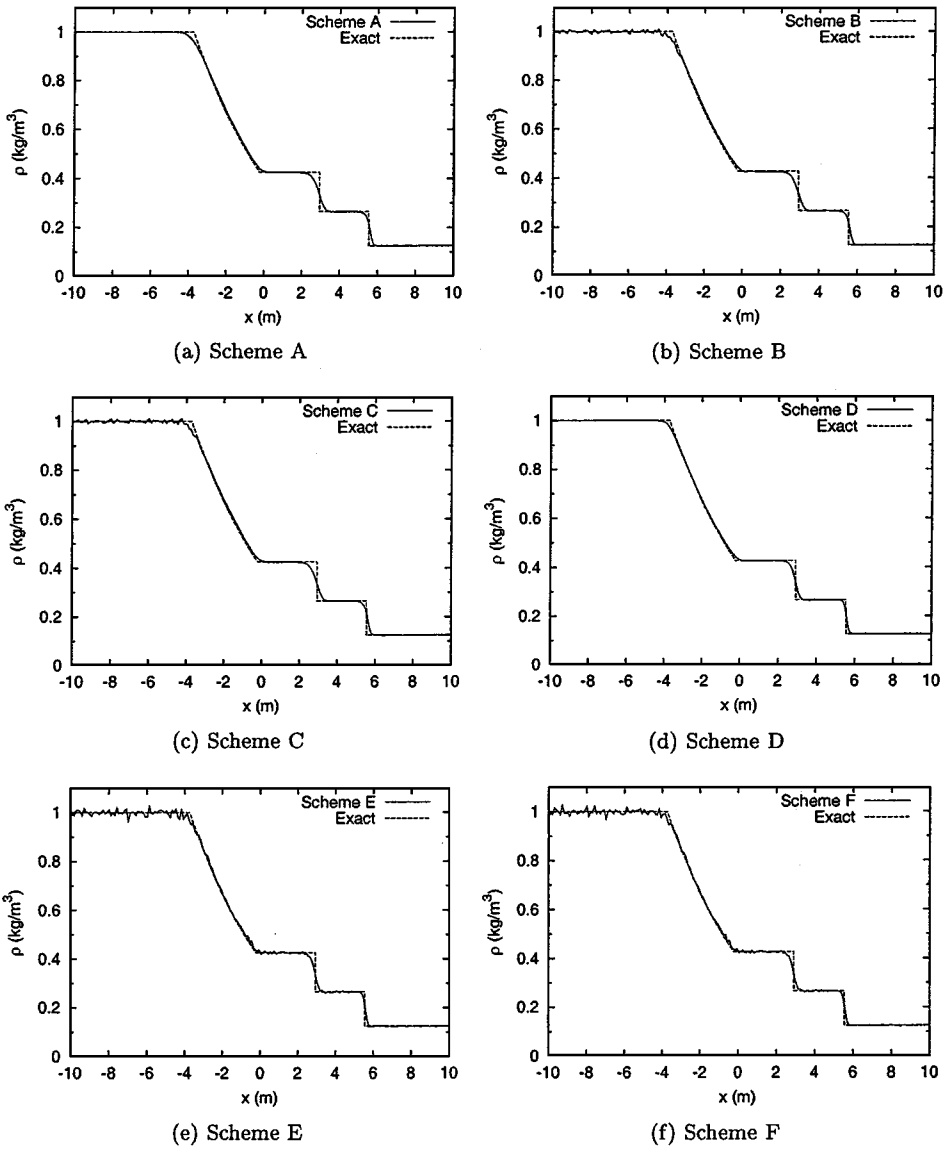

FIG. 2. Shock tube problem ($t = 10$ ms).

and particularly those that employ second-order time-discretization, exhibit bounded oscillations around an otherwise good solution, which is in agreement with the main theoretical result presented in this paper.

6.3. Aeroelastic Response of an F-16 Fighter

In order to highlight the impact of the theorems presented in this paper on industrial CFD applications, we simulate next the transient aeroelastic response to an initial disturbance of an F-16 fighter in transonic airstreams. We consider the following free-stream flow

conditions corresponding to a flight at an altitude of 10,000 ft:

$$M_\infty = 0.9$$
$$\rho_\infty = 1.02 \times 10^{-6} \text{ slugs/in}^3$$
$$p_\infty = 10.17 \text{ psi.}$$

We set the angles of attack to $\alpha = \beta = 0^\circ$. For this purpose, we construct a detailed finite element structural model of this aircraft featuring bar, beam, solid, plate, shell, metallic as well as composite elements, and a total of 168,799 degrees of freedom (see Fig. 3a). We discretize the surface of the F-16 with 63,044 grid points (see Fig. 3b) and generate a fluid volume mesh with 403,919 grid points.

We excite the F-16 by an initial disturbance of its aeroelastic equilibrium at the flight conditions specified above, and predict its subsequent transient aeroelastic response using

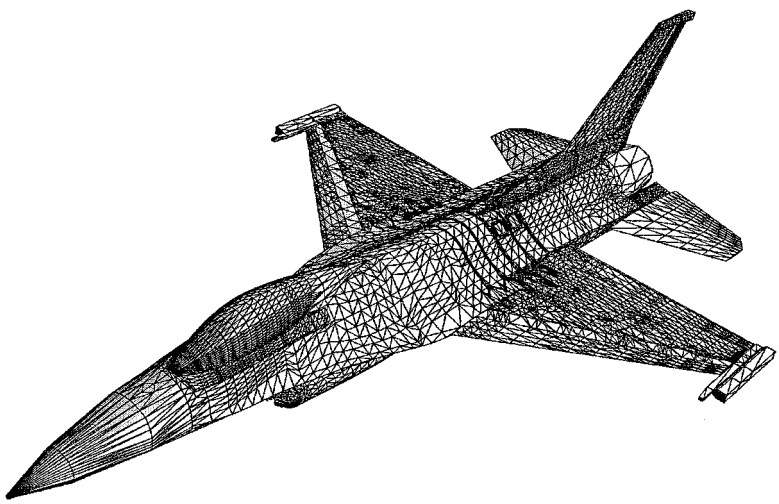

(a) Finite element structural model

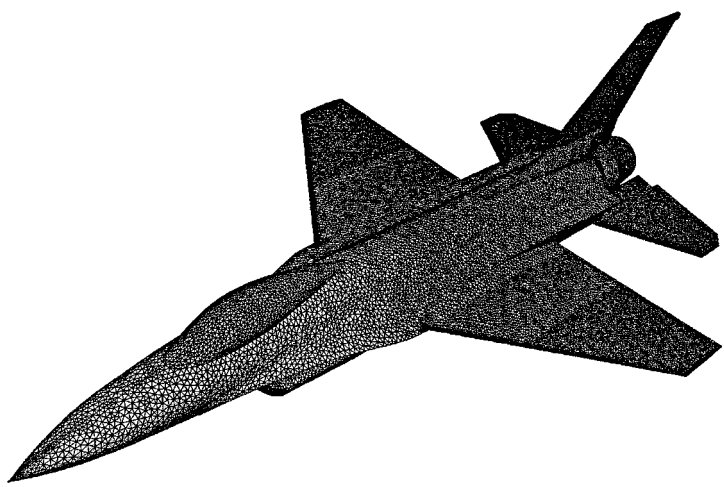

(b) Fluid surface grid

FIG. 3. Structural and fluid discretizations for the F-16 aeroelastic problem.

the partitioned procedure described in [19] for solving the coupled fluid/structure/mesh equations of motion. We equip this partitioned procedure with all of Scheme D, Scheme E, and Scheme F for solving the flow subproblem, and with the second-order unconditionally stable midpoint rule for time-integrating the structural motion. We assume that all modes that participate in this aeroelastic response are below 100 Hz—which is justified by the fact that the first and second natural modes of the F-16 are below 10 Hz—and therefore set the computational time step to $\Delta t = 1$ ms, which corresponds to sampling the frequency of 100 Hz in 10 points. This time step also turns out to be the maximum time step for which an acceptable accuracy can be obtained. We display in Fig. 4 some sample aeroelastic solutions, and report in Fig. 5 the lift histories computed using Scheme D, Scheme E, and Scheme F as flow solvers.

During the first 0.2 physical second, the same lift variation in time can be observed in all cases. Afterward, Scheme E and Scheme F appear to amplify the lift history. Using

(a) Von Mises stresses (amplified aeroelastic deformations)

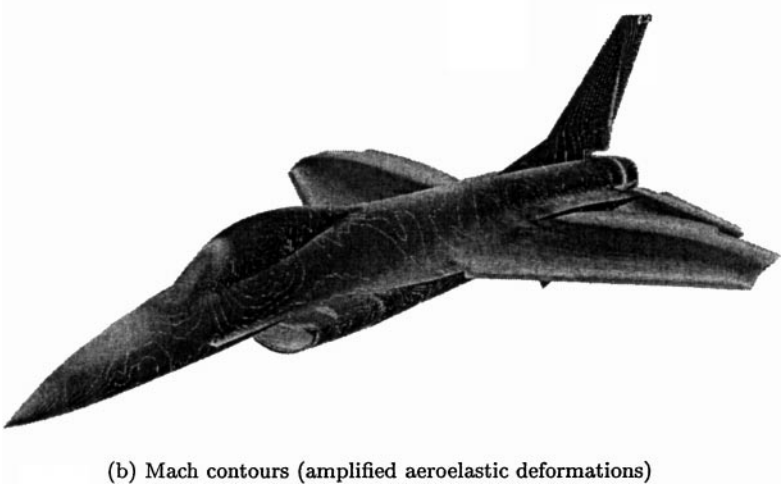

(b) Mach contours (amplified aeroelastic deformations)

FIG. 4. Sample solutions of the F-16 aeroelastic problem at $t = 0.6$ s.

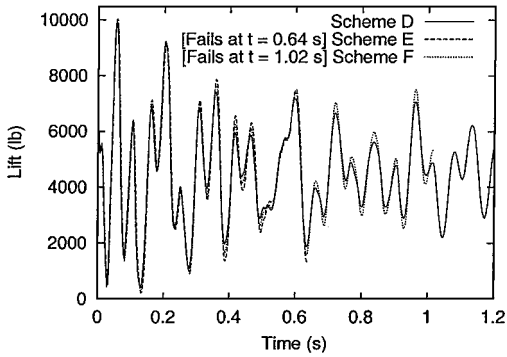

FIG. 5. Lift histories for the F-16 aeroelastic problem.

Scheme D, which satisfies its DGCL, the first 1.2 seconds of the aeroelastic response of the F-16 are predicted in 36 hours CPU on a 16-processor Origin 2000 system. Using Scheme E, which violates its DGCL, the numerical simulation fails at $t = 0.64$ s because of an instability in the flow solver. Using Scheme F, which also violates its DGCL, the simulation fails later at $t = 1.02$ s, again because of a numerical instability in the flow solver. These results are in agreement with the main theoretical result presented in this paper, and highlight the importance of the discrete geometric conservation law for real-life CFD applications on moving grids.

7. CONCLUSIONS

For each arbitrary Lagrangian Eulerian (ALE) or other numerical scheme designed for solving unsteady flow problems on moving grids, there exists a discrete geometric conservation law (DGCL) that governs its geometric parameters. From a physical viewpoint, this DGCL ensures that the given numerical scheme reproduces exactly a uniform flow. From a mathematical viewpoint, it is a necessary and sufficient condition for the given numerical scheme to preserve the nonlinear stability in the sense of the discrete maximum principle of its fixed grid counterpart. Hence, an ALE scheme which violates its DGCL is bound to exhibit spurious oscillations and overshoots for practical computational time steps. Occasionally, such a scheme can also exhibit an unbounded behavior. For these reasons, and because the computational overhead associated with enforcing a DGCL is minimal, we recommend numerical methods that satisfy their DGCLs when considering a CFD application on moving grids.

ACKNOWLEDGMENT

The first two authors acknowledge the support by the Air Force Office of Scientific Research under Grant F49620-99-1-0007.

REFERENCES

1. S. A. Morton, R. B. Melville, and M. R. Visbal, Accuracy and coupling issues of aeroelastic Navier-Stokes solutions of deforming meshes, AIAA Paper 97-1085, 38th AIAA Structures, presented at Structural Dynamics and Materials Conference, Kissimmee, Florida, April 7–10, 1997.

2. J. Donea, An Arbitrary Lagrangian-Eulerian finite element method for transient fluid-structure interactions, *Comput. Meth. Appl. Mech. Eng.* **33**, 689 (1982).
3. C. Farhat, M. Lesoinne, and N. Maman, Mixed explicit/implicit time integration of coupled aeroelastic problems: three-field formulation, geometric conservation and distributed solution, Internat. *J. Numer. Meth. Fluids* **21**, 807 (1995).
4. J. T. Batina, Unsteady Euler airfoil solutions using unstructured dynamic meshes, AIAA Paper 89-0115, presented at AIAA 27th Aerospace Sciences Meeting, Reno, Nevada, January 9–12, 1989.
5. H. Guillard and C. Farhat, On the significance of the geometric conservation law for flow computations on moving meshes, *Comput. Meth. Appl. Mech. Eng.* **190**, 1467 (2000).
6. P. D. Thomas and C. K. Lombard, Geometric conservation law and its application to flow computations on moving grids, *AIAA J.* **17**, 1030 (1979).
7. B. NKonga and H. Guillard, Godunov type method on non-structured meshes for three-dimensional moving boundary problems, *Comp. Meth. Appl. Mech. Eng.* **113**, 183 (1994).
8. M. Lesoinne and C. Farhat, Geometric conservation laws for flow problems with moving boundaries and deformable meshes, and their impact on aeroelastic computations, *Comput. Meth. Appl. Mech. Eng.* **34**, 71 (1996).
9. B. Koobus and C. Farhat, Second-order time-accurate and geometrically conservative implicit schemes for flow computations on unstructured dynamic meshes, *Comput. Meth. Appl. Mech. Eng.* **170**, 103 (1999).
10. L. Formaggia and F. Nobile, A stability analysis for the arbitrary Lagrangian Eulerian formulation with finite elements, *East-West J. Numer. Math.* **7**, 105 (1999).
11. J. P. Boris and D. L. Book, Flux-corrected transport I. SHASTA, a fluid transport algorithm that works, *J. Comput. Phys.* **11**, 38 (1973).
12. E. Godlewski and P. A. Raviart, Numerical Approximation of Hyperbolic Systems of Conservation Laws (Springer-Verlag, New York, 1996).
13. C. B. Laney, Computational Gas Dynamics (Cambridge Univ. Press, Cambridge, UK, 1998).
14. S. N. Kruzkhov, Generalized solutions of the Cauchy problem in the large for nonlinear equations of first order, *Dokl. Akad. Nauk. SSSR* **187**, 29 (1969).
15. C. Farhat, P. Geuzaine, and C. Grandmont, The discrete geometric conservation law and its effects on nonlinear stability and accuracy. AIAA Paper 2001-2607, presented at 15th AIAA Computational Fluid Dynamics Conference, Anaheim, California, June 11–14, 2001.
16. P. L. Roe, Approximate Riemann solvers, parameters vectors and difference schemes, *J. Comput. Phys.* **43**, 357 (1981).
17. B. Van Leer, Towards the ultimate conservative difference scheme V: A second-order sequel to Godunov's method, *J. Comput. Phys.* **32**, 361 (1979).
18. G. A. Sod, A survey of several finite difference methods for systems of nonlinear hyperbolic conservation laws, *J. Comput. Phys.* **27**, 1 (1978).
19. M. Lesoinne and C. Farhat, A higher-order subiteration free staggered algorithm for nonlinear transient aeroelastic problems, *AIAA J.* **36**, 1754 (1998).